Transfer of quantum states through a disordered channel with exponentially decaying couplings

F. J. Araujo Filho[1] · **R. F. Dutra**[1] · **I. F. F. dos Santos**[1] · **M. L. Lyra**[1] · **G. M. A. Almeida**[1] · **F. A. B. F. de Moura**[1]

Abstract

The transmission of a qubit in a tight-binding channel with exponentially decaying hopping terms and diagonal disorder is investigated. The end sites act as sender and receiver and are perturbatively coupled to the channel. This is done to suppress interference of the channel modes during the time evolution of the state. We explore the performance of the transfer fidelity against the disorder strength and hopping range within the channel. The scaling behavior of the participation number as a function of the hopping range is also discussed. Channels featuring long-range interactions display distinct robustness against disorder and high-quality quantum state transfer is attainable even for disorder levels of the order of the largest hopping amplitude.

1 Introduction

In recent years, theoretical and experimental research on quantum information processing have become a very active topic in a range of fields. A current challenge is to develop robust quantum devices able to handle several qubits with an error rate below an acceptable threshold [1]. Among many tasks, quantum processors must perform quantum state transfer (QST) protocols from one location to another with high fidelity [2, 3]. Quantum networks are often designed in hybrid light-matter platforms [4] so as to make use of advanced photonic technology. However, the frequent conversion between stationary and flying qubits can lead to decoherence [5]. Alternatively, minimum-control QST protocols can operate on engineered spin chains evolving via their Hamiltonian dynamics up to a specified time. This idea was put forward by Bose

✉ G. M. A. Almeida
  gmaalmeida@fis.ufal.br

1   Instituto de Física, Universidade Federal de Alagoas, Maceió, Alagoas 57072-970, Brazil

⁇ Springer

in Ref. [6], where a simple uniform chain was shown to provide with better-than-classical fidelities at short distances. Coupled spin$-1/2$ chains with interactions have since been explored in many forms, each with its own speed-fidelity merit [7–24].

A way to perform long-distance quantum communication is to harness the symmetry of the lattice and set about edge states having negligible overlap with the bulk. This can be done by, e.g. applying strong magnetic fields close the sender and receiver [19, 21] and by setting perturbative end couplings [9, 10]. These configurations are often robust against noise as they do not rely on strict engineering schemes [25]. Modified structures such as the dimerized Su-Schrieffer-Heeger chain can offer extra topological protection [26] with the cost of having longer transfer times τ [22, 27]. In Rabi-like QST protocols one has $\tau \propto g^{-2}$ with the fidelity scaling as $1 - O(g^2)$, g being the perturbation parameter [10]. Recently, a dimerized chain with time-dependent next-to-nearest-neighbor couplings has been proposed as a much faster alternative while also being robust against uncorrelated and correlated disorder [28]. The manipulation of parameters associated with correlations in the disorder distributions [29–33] have been recently explored concerning a potential impact on the quantum state transfer efficiency. This feature is directly related to the influence of disorder correlations on the localized/delocalized nature of quantum states [34–36].

Spin chains featuring long-range interactions can also host high-fidelity QST [14, 24]. A non-isotropic Heisenberg XXZ chain has recently been investigated in which the couplings decay as a power-law featuring a tunable exponent and symmetrically coupled sender and receiver sites [24]. It is shown that an increase in the dimensionality of the system can result in an effective end-to-end coupling resulting in Rabi-like oscillations [24]. In addition, they suffer less from temperature-induced disorder compared to chains with nearest-neighbor couplings only [24]. However, although power-law decaying interactions arise in some specific physical systems such as those with dipolar interactions [37, 38], tight-binding hopping amplitudes depict an exponential decay with distance in general condensed matter systems with screened interactions. This results from the typical exponential decay of the localized atomic orbitals that imposes a similar decay to the exchange integrals involved in the hopping amplitude calculation.

Those and other results establish that the topology of the channel plays a crucial role in the quality of a QST protocol running in the Rabi regime [27]. In this work, we explore in detail the localization properties of a channel displaying exponentially-decaying hopping amplitudes $\propto e^{-\nu r}$ commonly found in condensed matter systems. The exponential decay of the couplings is not able to induce an effective higher dimensionality of the system as it occurs in the presence of power-law decaying interactions [37]. Therefore, no extended states are supported by the system in the thermodynamic limit. However, the relation of the relevant length scales associated with the system size, localization length and typical range of the interaction is expected to determine distinc quantum state transfer regimes. The decay rate with distance r is controlled by a single parameter ν which in the limit $\nu \to \infty$ renders the usual 1D configuration with nearest-neighbor interactions. We seek for the energy range within the channel spectrum where the highest fidelity can be obtained when two end spins are weakly attached to it. Remarkably, even when the diagonal disorder strength is a few times larger than the maximum hopping amplitude ($\equiv 1$) fidelities above 0.9 are obtained

given ν is low enough. Under these terms, long-range spin chains are preferable to standard, nearest-neighbor 1D models.

2 Hamiltonian model

Consider a onedimensional spin-1/2 chain with open boundary conditions composed of $N + 2$ particles coupled via XX interactions. In the single-excitation subspace spanned by $|n\rangle \equiv |0\rangle^{\otimes n-1} |1\rangle |0\rangle^{\otimes N+2-n}$ ($n = 1, \ldots, N + 2$), the system can be expressed as a tight-binding Hamiltonian of the form

$$H = \sum_{n=1}^{N+2} \epsilon_n |n\rangle\langle n| + \sum_{n,m;n\neq m} J_{n,m} |n\rangle \langle m|, \tag{1}$$

where ϵ_n are the on-site energies and $J_{n,m} = J_{m,n}$ are the hopping amplitudes. The sender and receiver are represented by sites 1 and $N + 2$, respectively. Sites 2 through $N + 1$ then form the channel.

Let us now consider that the communicating parties are coupled to the channel via $J_{1,2} = J_{N+1,N+2} = g$ whereas the amplitudes within the channel decay exponentially as

$$J_{n,m} = \exp[-\nu(r_{n,m} - 1)], \tag{2}$$

where $r_{n,m} = |n-m|$ represents the distance between sites n and m, with $1 < n(m) < (N + 2)$ and $n \neq m$. The decay parameter ν is such that its inverse sets the typical range of the interaction. Nearest-neighbor amplitudes read $J_{n,n+1} = J \equiv 1$ and set our reference energy scale.

As commented above, such decay law of the hopping amplitudes usually takes place in condensed matter systems with screened short-range interactions due the exponentially localized character of the atomic orbitals involved in the exchange coupling interactions. Contrasting with one-dimensional systems having power-law decaying couplings that can effectively behave as a higher dimensional system with short-range couplings [37], the exponential decay law of the hopping amplitudes does not change the one-dimensional character of the system. As such, all states remain exponentially localized in the thermodynamic limit. In finite chains, it is the relation between the three relevant scale lengths (system size, localization length, and typical decay length of the interactions) that will ultimately determine the distinct regimes of localization and, consequently, govern the efficiency of the QST.

We will work in the weak coupling regime where $g \ll 1$ so as to induce resonant Rabi-like oscillations between sites 1 and $N + 2$ [9]. Now, the local energies of the communicating spins are also set as a tunable parameter $\epsilon_1 = \epsilon_{N+2} = \omega$. It will be used to screen the spectrum of the channel to optimize the transfer fidelity [39]. The on-site energies within the channel ϵ_n ($n = 2, \ldots, N + 1$) are uncorrelated random numbers uniformly distributed within the range $[-W/2, W/2]$, where W stands for the disorder strength. Our goal here is to test the QST performance against W for a
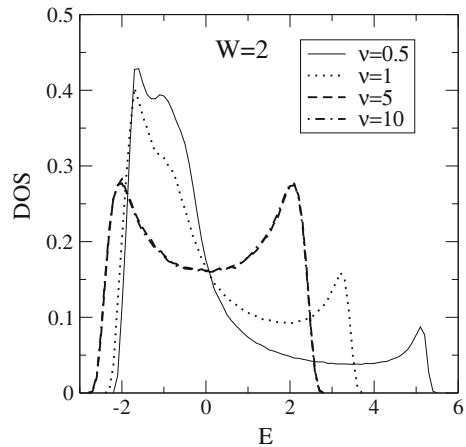
range of ν and ω values. Before that, though, we discuss the localization profile of the channel in the following section.

3 Results

3.1 Localization properties

Our analysis is entirely done via exact diagonalization of the Hamiltonian in Eq. (1). For now, let us take sites 1 and $N + 2$ aside ($g = 0$) and focus only on the channel modes (spanned by states $|2\rangle$ through $|N + 1\rangle$).

We begin by measuring the density of states defined by $DOS = \sum_k \delta(E - E_k)$, where E_k are the eigenvalues of the channel. Results are depicted in Fig. 1 for $\nu = 0.5, 1, 5, 10$ and $W = 2$. We readily see that for large ν we approach the usual profile of a 1D lattice with neareast-neighbor hoppings. For small ν, the DOS exhibits an asymmetric form which is typical of long-range hopping models.

To quantify localization along the spectrum we evaluate participation number defined as

$$P(E_k) = \left[\sum_n (z_n^{(k)})^4 \right]^{-1}, \tag{3}$$

for a given eigenvalue E_k, where $z_n^{(k)} = \langle n|E_k \rangle$ is the corresponding wavefunction at n. The participation number diverges with N for extended states. If the state is localized, then it remains constant and shall significantly impact the QST when the typical localization length is much smaller than the system size [39].

Figure 2 shows the resulting participation number averaged over 300 independent realizations of disorder. Due to the fluctuations the participation number is averaged out over small energy intervals as $P(E) = \sum_{|E_k - E| < \Delta E} P(E_k)/N_E$, with $\Delta E = 0.1$
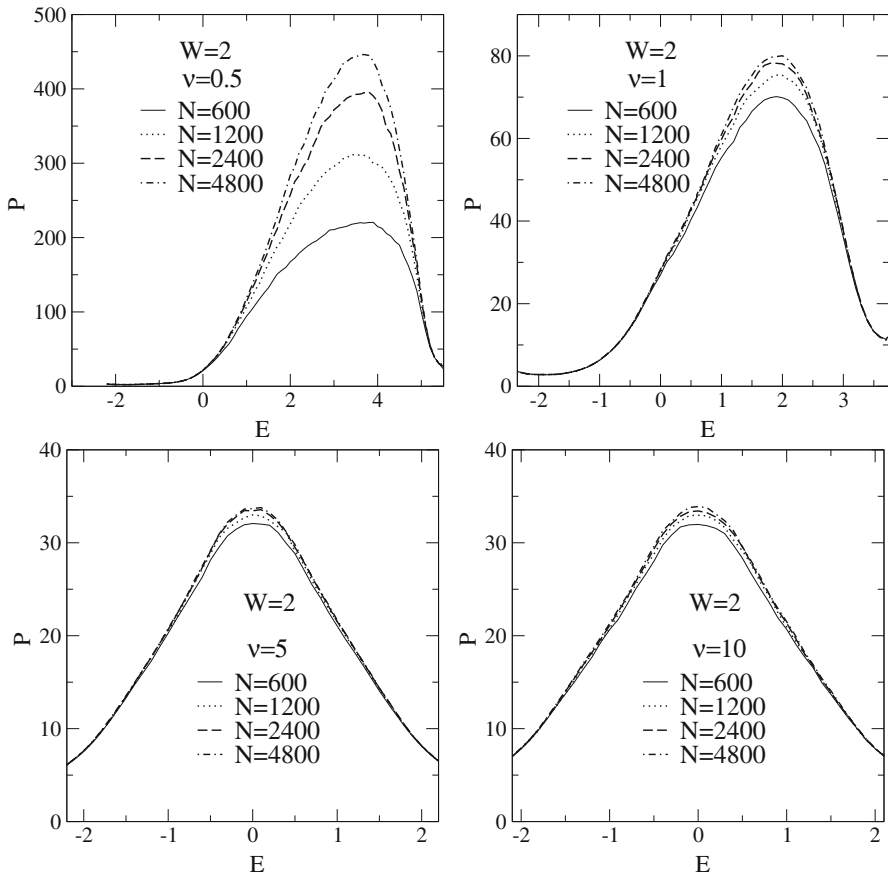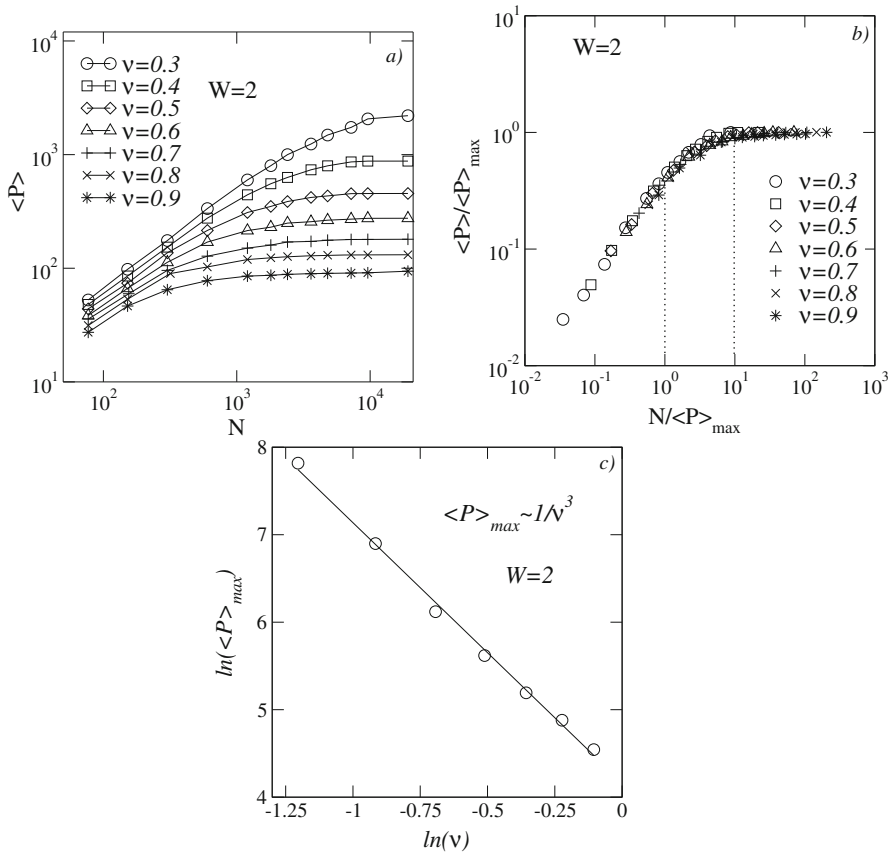
Fig. 2 Average participation number $P(E)$ versus energy E for $\nu = 0.5, 1, 5, 10$, with $W = 2$. States populating higher energies are significantly less localized for slowly decaying hopping amplitudes

and N_E being the number of states with having between $E - \Delta E$ and $E + \Delta E$. For higher values of ν, the participation number is almost insensitive to N, which is the expected outcome for uncorrelated disordered 1D systems. That is when Anderson localization effects take over.

In contrast, for small values of ν the participation number, besides displaying an asymmetric profile, is largely affected by the size N at higher energy levels (see the curves for $\nu = 0.5$ at $E \approx 3.5$ in Fig. 2).

We now compute the average participation number $\langle P \rangle$ and observe it against the system size N in Fig. 3a for several values of ν. They suggest that for large N maximum participation number saturates and this points out to the existence of localized states. To see it further, we proceed with a finite-size scaling. In each case we rescale the participation number by its maximum $\langle P \rangle_{max}$ and the system size N by the same amount. This results in the data collapse shown in Fig. 3b. Such a procedure is based on the single-parameter scaling hypothesis. According to that, the

Fig. 3 **a** Average participation number $\langle P \rangle$ versus N for $\nu = 0.3$ up to 0.9, with fixed $W = 2$. **b** Collapse of the previous data using the rescaled variable $\langle P \rangle / \langle P \rangle_{\max}$ as a function of $N / \langle P \rangle_{\max}$. **c** The characteristic localization length $\langle P \rangle_{\max}$ scales as $1/\nu^3$

average participation number can be written as $\langle P \rangle (N, \nu) = P_{\max}(\nu) f[N/P_{\max}(\nu)]$, where $P_{\max}(\nu)$ represents the typical average localization length. For $N/P_{\max} \gg 1$, the scaling function $f[N/P_{\max}(\nu)]$ converges to unit. In contrast, for short chains $N/P_{\max} \ll 1$, $f[N/P_{\max}(\nu)] \propto N/P_{\max}(\nu)$ rendering the average participation to grow linearly with N, as expected in the regime of negligible disorder.

In Fig. 3c we obtain $P_{\max} \approx 1/\nu^3$ for a range of small ν values.

From the analysis above we can conclude that the channel does not host strict extended states in the thermodynamic limit. However, our calculations indicate that an increase in the hopping range (small ν) suppresses the localization degree (as readily seen from the increase of the participation number in Fig. 2). This fact can be useful in the context of QST through finite channels, particularly for sizes of the same order of the typical localization length.
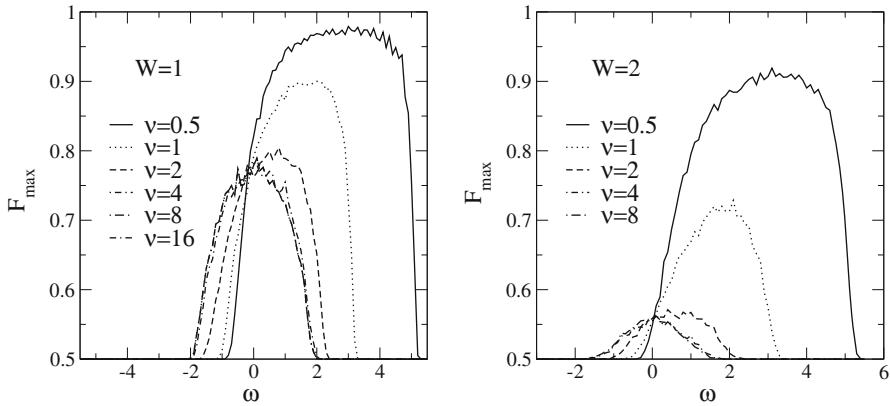
Fig. 4 Maximum fidelity versus ω for $N = 100$, considering $v = 0.5, 1, 2, 3, 4, 8$, $W = 1, 2$, and fixed $g = 0.01$. F_{max} is averaged over 100 independent realizations of disorder. Note that QST performance is greatly improved for lower values of v.

3.2 Quantum state transfer

We are now ready to investigate the single-particle dynamics through the chain. Our primary interest is to assess the performance of transmission of a single qubit from site 1 to site $N + 2$ (we are now back to the full form of the Hamiltonian in Eq. (1)).

An arbitrary qubit with amplitudes α and β prepared at the first site while setting all the remaining sites at the zero (spin down) state forms the initial state $|\psi(t = 0)\rangle = \alpha |vac\rangle + \beta |1\rangle$, where $|vac\rangle \equiv |0\rangle^{\otimes N+2}$. The goal is to recover the same qubit state at the last site $N + 2$. The proper measure of performance here is the transmission fidelity averaged over all possible input values (α, β), i.e., over the Bloch sphere (of radius $|\alpha|^2 + |\beta|^2 = 1$). The so-called averaged fidelity reads [6]

$$F(t) = \frac{1}{2} + \frac{|c_{N+2}(t)|}{3} + \frac{|c_{N+2}(t)|^2}{6}, \tag{4}$$

where $c_{N+2}(t) = \langle N + 2|e^{-iHt}|1\rangle$ is the transition amplitude from site 1 to site $N + 2$ due to the quantum time evolution operator. In the formula above we are effectively taking $\arg\{c_{N+2}(t)\} = 0$ at the arrival time, which can be realized by applying a local rotation to the last spin. A well defined Rabi-like scenario in our protocol is implied by the occurrence of a pair of eigenstates $\sim (|1\rangle \pm |N + 2\rangle)/\sqrt{2}$. That renders a fidelity close to unit, with the worst case scenario being $F = 1/2$.

The transfer time for Rabi-like QST protocols is $\tau = \pi/\delta$, where δ is the small gap $\propto g^2$ between the edge modes. Due to disorder, τ will fluctuate. For now, instead of evaluating the fidelity at a specific time we present the maximum fidelity F_{max} obtained from $t = 0$ up to $t = 100 \times g^{-2}$. This ultimately allows us to estimate the quality of the QST. Unless stated otherwise, the numerical simulations in the following are performed for 100 independent realizations of disorder, with $N = 100$ and $g = 0.01$.

Fig. 5 Maximum fidelity versus the disorder strength W for distinct values of ν, with $N = 100$ and $g = 0.01$
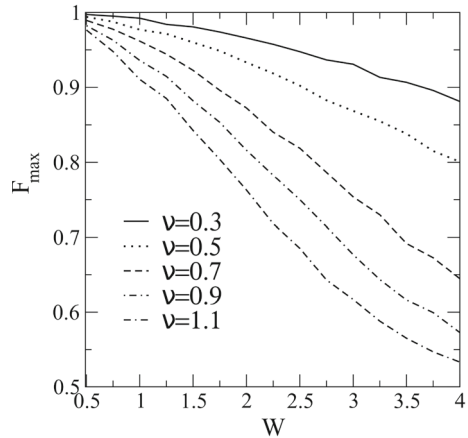

In Fig. 4 we plot $F_{\max}$ versus the on-site energy $\omega = \epsilon_1 = \epsilon_{N+2}$ for several exponents ν and distinct disorders strengths W. We see that for large ν, the QST is largely affected by the disorder, yielding fidelities way bellow the classical threshold $F = 2/3$ [6] when $W = 2$. Indeed, Zwick *et al.* found that various nearest-neightbor 1D configurations obey the scaling law $F = \frac{1}{2}(1 + e^{-aNW^b})$, with a and b being fitting parameters [25]. Even as weak-coupling models typically offer better resilience against disorder compared to other schemes, $W = 2$ is beyond tolerable. On the other hand, the QST performance gets a tremendous boost (offering $F > 0.9$) for lower values of ν even at that disorder levels as high as $W \approx 4$ (see Fig. 5). Recall that the maximum hopping amplitude is $J \equiv 1$.

Figure 4 also highlights the role of the local energy ω. The fidelity is maximized whenever ω meets an energy range mostly populated by modes having larger localization lengths [cf. Fig. 2]. This indicates that a proper effective resonant two-level (Rabi) regime calls for delocalized eigenstates with energies close to ω or else a detuned Rabi dynamics is achieved (even as $g \to 0$) [27].

In Fig. 6 we show the probability distribution $P(F_{\max})$ for $W = 1$ and $W = 2$. This is done for ω fixed at levels that provide the best QST performances. For example, we pick $\omega = 4$ for $\nu = 0.3$ and $W = 2$. We indeed confirm that for small values of ν, it is most likely to obtain $F(\tau) \approx 1$.

The QST analysis so far has been based on the evaluation of the fidelity within a broad time window. While it offers a good figure of merit, any QST protocol in reality requires a pre-established measurement time. Timing errors will naturally be present due to the fluctuations occurring in the gap δ. The disorder can also shift the energies of the channel modes toward ω. In this case, the Rabi-like framework is compromised unless $g \to 0$. A perfect resonance between ω and some channel mode will eventually lead to an effective three-level dynamics and may also suit for QST albeit in a distinct timescale [9].
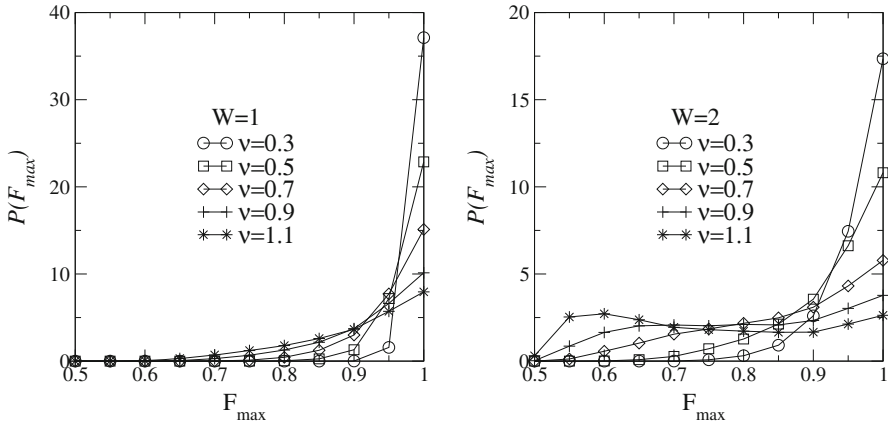
Fig. 6 Probability distribution $P(F_{max})$ for $W = 1$ and $W = 2$ at appropriate tuning energies ω that allow for optimal QST performances

Fig. 7 QST timescale parameter $|\Lambda|$ versus ν for $N = 50$, $W = 0$, and $\omega = 0$. In the limit of nearest-neighbor interactions $|\Lambda| \to 1$
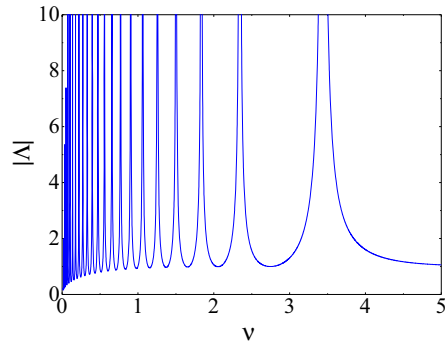

In Rabi-like QST protocols, the transfer time is $\tau = \tau/\delta$, with $\delta = 2g^2|\Lambda|$, where

$$\Lambda = \sum_k \frac{z_2^{(k)} z_{N+1}^{(k)*}}{E_k - \omega} \tag{5}$$

is obtained via perturbation theory applied to the channel Hamiltonian [9, 27]. For 1D channels with nearest-neighbor interactions, $|\Lambda| = 1$ (in units of $1/J$) [9, 27] given ω lies at the center of the band. In Fig. 7 we display this parameter against ν for $\omega = 0$ and $W = 0$. All the spikes in the curve indicate resonant points where $E_k = \omega$ for some k. In other words, Λ diverges. As a consequence, the effective Rabi dynamics ceases to hold. The number of these singularities and their corresponding values of ν vary with N. Note that $|\Lambda| \to 1$ as ν grows, as expected.

Once the channel parameter Λ is known for the ideal scenario ($W = 0$), the transfer time τ can be prescribed. Let us finally see how the fidelity $F(\tau)$ behaves in the presence of disorder. Figure 8 shows the results against ν for distinct disorder strengths W and tuning energies ω. When $\omega = 0$ [Fig. 8a] the fidelity drops rapidly upon

(a)

(b)
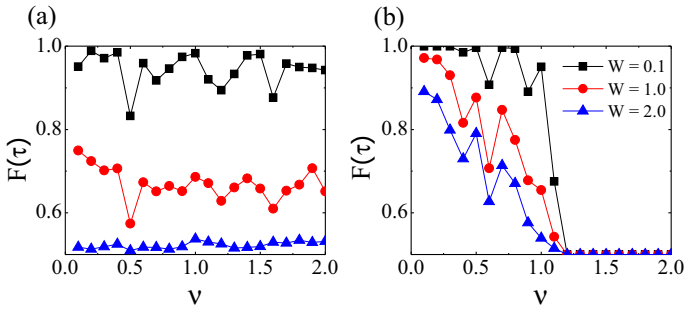
Fig. 8 Averaged fidelity $F(\tau)$ versus ν evaluated at the expected time $\tau = \pi/(2g^2|\Lambda|)$, with Λ defined for $W = 0$. Tuning energies are **a** $\omega = 0$ and **b** $\omega = 3$ for $N = 100$ and $g = 0.01$. Various disorder strengths W are considered and the curves are averaged over 100 independent realizations of disorder

increasing W for any ν. Yet, moderate values of disorder should provide with fidelities above the classical threshold $F = 2/3$ [6]. Now, when ω is set more conveniently [$\omega = 3$ in Fig. 8b] the fidelity is quite robust against disorder and also timing errors up to $\nu = 1$. Above this level, the fidelity sharply decays. Surprisingly, even when $W = 1$ the fidelity evaluated at the expected time τ is close to unit given ν is low enough. We remark the unstable behavior of $F(\tau)$ in Fig. 8 is largely due to the proximity between ω and some E_k (given $g = 0.01$ is fixed), as ν varies.

4 Conclusions

Some degree of disorder will always be present in engineered solid-state devices for quantum communication protocols. It may manifest as fluctuations in the static parameters of the network. Therefore, any quantum communication protocol should take that into account [25].

We have put forward a high-fidelity QST protocol on a tight-binding chain featuring hopping amplitudes decaying exponentially in the presence of significant levels of disorder. Long-range interactions generally increases the number of pathways to delocalization and play a crucial role in other phenomena such as many body localization [37]. While power-law decaying couplings may lead to an effective increase in the system dimensionality and promote the emergence of extended states [37], linear systems with exponentially decaying couplings are intrinsically unidimensional with all states remaining localized in the thermodynamic limit. However, the localization length of the one-particle eigenstates are affected by the typical decay length of the interactions, thus dictating the quality of the QST on finite chains.

The presence of channel modes displaying larger localization length in some energy range in the channel spectrum maximizes the chances of establishing an effective resonant Rabi-like interaction between the end points of the chain. This ultimately renders $F \approx 1$ when the hopping strength exponent ν is small enough. We unveiled that average maximum participation number (working as a measure of localization) scales as $1/\nu^3$ for small values of ν. Therefore, when the localization length becomes signif-

icantly large, proper tuning of the local sender/receiver energies provides a robust, high-quality qubit transfer.

Data availibility The datasets generated during and/or analysed during the current study are available from the corresponding author on reasonable request.

Declarations

Conflict of interests The authors have no relevant financial or non-financial interests to disclose.

References

1. Preskill, J.: Quantum Computing in the NISQ era and beyond. Quantum, 2, 79 (2018) https://doi.org/10.22331/q-2018-08-06-79
2. Apollaro, T.J.G., Lorenzo, S., Plastina, F.: Transport of quantum correlations across a spin chain. Int. J. Mod. Phys. B **27**, 1345035 (2013). https://doi.org/10.1142/S0217979213450355
3. Kay, A.: Perfect, efficient, state transfer and its application as a constructive tool. Int. J. Quantum Inf. **08**, 641 (2010). https://doi.org/10.1142/S0219749910006514
4. Kimble, H.J.: The quantum internet. Nature **453**, 1023 (2008). https://doi.org/10.1038/nature07127
5. Lu, J., Zhou, L., Fu, H.C., Kuang, L.-M.: Quantum decoherence in a hybrid atom-optical system of a one-dimensional coupled-resonator waveguide and an atom. Phys. Rev. A **81**, 062111 (2010). https://doi.org/10.1103/PhysRevA.81.062111
6. Bose, S.: Quantum communication through an unmodulated spin chain. Phys. Rev. Lett. **91**, 207901 (2003). https://doi.org/10.1103/PhysRevLett.91.207901
7. Christandl, M., Datta, N., Ekert, A., Landahl, A.J.: Perfect state transfer in quantum spin networks. Phys. Rev. Lett. **92**, 187902 (2004). https://doi.org/10.1103/PhysRevLett.92.187902
8. Plenio, M.B., Hartley, J., Eisert, J.: Dynamics and manipulation of entanglement in coupled harmonic systems with many degrees of freedom. New J. Phys. **6**(1), 36 (2004). https://doi.org/10.1088/1367-2630/6/1/036
9. Wójcik, A., Łuczak, T., Kurzynski, P., Grudka, A., Gdala, T., Bednarska, M.: Unmodulated spin chains as universal quantum wires. Phys. Rev. A **72**, 034303 (2005). https://doi.org/10.1103/PhysRevA.72.034303
10. Wójcik, A., Łuczak, T., Kurzynski, P., Grudka, A., Gdala, T., Bednarska, M.: Multiuser quantum communication networks. Phys. Rev. A **75**, 022330 (2007). https://doi.org/10.1103/PhysRevA.75.022330
11. Li, Y., Shi, T., Chen, B., Song, Z., Sun, C.-P.: Quantum-state transmission via a spin ladder as a robust data bus. Phys. Rev. A **71**, 022301 (2005). https://doi.org/10.1103/PhysRevA.71.022301
12. Huo, M.X., Li, Y., Song, Z., Sun, C.P.: The Peierls distorted chain as a quantum data bus for quantum state transfer. Europhys. Lett. **84**, 30004 (2008). https://doi.org/10.1209/0295-5075/84/30004
13. Liu, J., Zhang, G.-F., Chen, Z.-Y.: Quantum state transfer via a two-qubit Heisenberg XXZ spin model. Phys. Lett. A **372**(16), 2830 (2008). https://doi.org/10.1016/j.physleta.2008.01.017
14. Gualdi, G., Kostak, V., Marzoli, I., Tombesi, P.: Perfect state transfer in long-range interacting spin chains. Phys. Rev. A **78**, 022325 (2008). https://doi.org/10.1103/PhysRevA.78.022325
15. Wang, Z.-M., Byrd, M.S., Shao, B., Zou, J.: Quantum communication through anisotropic Heisenberg XY spin chains. Phys. Lett. A **373**(6), 636 (2009). https://doi.org/10.1016/j.physleta.2008.12.016
16. Banchi, L., Apollaro, T.J.G., Cuccoli, A., Vaia, R., Verrucchi, P.: Optimal dynamics for quantum-state and entanglement transfer through homogeneous quantum systems. Phys. Rev. A **82**, 052321 (2010). https://doi.org/10.1103/PhysRevA.82.052321
17. Banchi, L., Apollaro, T.J.G., Cuccoli, A., Vaia, R., Verrucchi, P.: Long quantum channels for high-quality entanglement transfer. New J. Phys. **13**(12), 123006 (2011). https://doi.org/10.1088/1367-2630/13/12/123006

18. Apollaro, T.J.G., Banchi, L., Cuccoli, A., Vaia, R., Verrucchi, P.: 99%-fidelity ballistic quantum-state transfer through long uniform channels. Phys. Rev. A **85**, 052319 (2012). https://doi.org/10.1103/PhysRevA.85.052319

19. Lorenzo, S., Apollaro, T.J.G., Sindona, A., Plastina, F.: Quantum-state transfer via resonant tunneling through local-field-induced barriers. Phys. Rev. A **87**, 042313 (2013). https://doi.org/10.1103/PhysRevA.87.042313

20. Paganelli, S., Lorenzo, S., Apollaro, T.J.G., Plastina, F., Giorgi, G.L.: Routing quantum information in spin chains. Phys. Rev. A **87**, 062309 (2013). https://doi.org/10.1103/PhysRevA.87.062309

21. Lorenzo, S., Apollaro, T.J.G., Paganelli, S., Palma, G.M., Plastina, F.: Transfer of arbitrary two-qubit states via a spin chain. Phys. Rev. A **91**, 042321 (2015). https://doi.org/10.1103/PhysRevA.91.042321

22. Almeida, G.M.A., Ciccarello, F., Apollaro, T.J.G., Souza, A.M.C.: Quantum-state transfer in staggered coupled-cavity arrays. Phys. Rev. A **93**, 032310 (2016). https://doi.org/10.1103/PhysRevA.93.032310

23. Apollaro, T.J.G., Almeida, G.M.A., Lorenzo, S., Ferraro, A., Paganelli, S.: Spin chains for two-qubit teleportation. Phys. Rev. A **100**, 052308 (2019). https://doi.org/10.1103/PhysRevA.100.052308

24. Hermes, S., Apollaro, T.J.G., Paganelli, S., Macrì, T.: Dimensionality-enhanced quantum state transfer in long-range-interacting spin systems. Phys. Rev. A **101**, 053607 (2020). https://doi.org/10.1103/PhysRevA.101.053607

25. Zwick, A., Álvarez, G.A., Stolze, J., Osenda, O.: Quantum state transfer in disordered spin chains: how much engineering is reasonable? Quant. Inf. Comp. **15**, 852 (2015). https://doi.org/10.26421/QIC15.7-8-4

26. Giampaolo, S.M., Illuminati, F.: Long-distance entanglement in many-body atomic and optical systems. New J. Phys. **12**, 025019 (2010). https://doi.org/10.1088/1367-2630/12/2/025019

27. Almeida, G.M.A.: Interplay between speed and fidelity in off-resonant quantum-state-transfer protocols. Phys. Rev. A **98**, 012334 (2018). https://doi.org/10.1103/PhysRevA.98.012334

28. D'Angelis, F.M., Pinheiro, F.A., Guéry-Odelin, D., Longhi, S., Impens, F.M.C.: Fast and robust quantum state transfer in a topological Su-Schrieffer-Heeger chain with next-to-nearest-neighbor interactions. Phys. Rev. Res. **2**, 033475 (2020). https://doi.org/10.1103/PhysRevResearch.2.033475

29. Almeida, G.M.A., Moura, F.A.B.F., Lyra, M.L.: Transmission of quantum states through disordered channels with dimerized defects. Quant. Inf. Proc. **18**, 350 (2019). https://doi.org/10.1007/s11128-019-2464-6

30. Almeida, G.M.A., Souza, A.M.C., de Moura, F.A.B.F., Lyra, M.L.: Robust entanglement transfer through a disordered qubit ladder. Phys. Lett. A **383**(27), 125847 (2019). https://doi.org/10.1016/j.physleta.2019.125847

31. Almeida, G.M.A., Moura, F.A.B.F., Apollaro, T.J.G., Lyra, M.L.: Disorder-assisted distribution of entanglement in XY spin chains. Phys. Rev. A **96**, 032315 (2017). https://doi.org/10.1103/PhysRevA.96.032315

32. Júnior, P.R.S., Almeida, G.M.A., Lyra, M.L., de Moura, F.A.B.F.: Quantum communication through chains with diluted disorder. Phys. Lett. A **383**(16), 1845–1849 (2019). https://doi.org/10.1016/j.physleta.2019.03.010

33. Messias, D., Mendes, C.V.C., Almeida, G.M.A., Lyra, M.L., de Moura, F.A.B.F.: Rabi-like quantum communication in an aperiodic spin-1/2 chain. J. Magn. Magn. Mater. **505**, 166730 (2020). https://doi.org/10.1016/j.jmmm.2020.166730

34. Moura, F.A.B.F., Lyra, M.L.: Delocalization in the 1d Anderson model with long-range correlated disorder. Phys. Rev. Lett. **81**, 3735–3738 (1998). https://doi.org/10.1103/PhysRevLett.81.3735

35. Mendes, C.V.C., Almeida, G.M.A., Lyra, M.L., Moura, F.A.B.F.: Localization-delocalization transition in discrete-time quantum walks with long-range correlated disorder. Phys. Rev. E **99**, 022117 (2019). https://doi.org/10.1103/PhysRevE.99.022117

36. Mendes, C.V.C., Almeida, G.M.A., Lyra, M.L., de Moura, F.A.B.F.: Localization properties of a discrete-time 1D quantum walk with generalized exponential correlated disorder. Phys. Lett. A **394**, 127196 (2021). https://doi.org/10.1016/j.physleta.2021.127196

37. Burin, A.L.: Localization in a random XY model with long-range interactions: intermediate case between single-particle and many-body problems. Phys. Rev. B **92**, 104428 (2015). https://doi.org/10.1103/PhysRevB.92.104428

38. Malyshev, A.V., Malyshev, V.A., Dominguez-Adame, F., Rodriguez, A.: Universal parameter at the Anderson transition on a one-dimensional lattice with non-random long-range coupling. J. Lumin. **108**, 269 (2004). https://doi.org/10.1016/j.jlumin.2004.01.057

39. Almeida, G.M.A., Moura, F.A.B.F., Lyra, M.L.: High-fidelity state transfer through long-range corre-lated disordered quantum channels. Phys. Lett. A **382**, 1335 (2018). https://doi.org/10.1016/j.physleta.2018.03.028